Journal of Engineering Sciences
Vol 11, Issue 8, August/2020
ISSN NO:0377-9254

A Successive Double Layer Wideband Antenna Using TDF Around 20 GHz

T.Prasanna[1], M. Gnanapriya[2]

#1PG Scholar,Dept Of ECE, Gokula Krishna College of Engineering, Nellore,AP,India.

#2Associate Professor&HOD ,Dept Of ECE, Gokula Krishna College of Engineering, Nellore,AP,India.

ABSTRACT_

A double layer wideband transmit exhibit recieving wire utilizing two degrees of opportunity components is introduced. The twofold layer transmit exhibit recieving wire is made out of 441 components. Every component incorporates four metal vias and two patches with two degrees of opportunity (TDF) imprinted on the two sides of the dielectric substrate. Four metal vias are utilized to accomplish the most extreme transmission greatness and two patches with TDF are embraced to acquire an adequately huge variety scope of stage move. A square transmit exhibit is structured, manufactured, and estimated to approve the proposed plan. Reenactment and estimation results have great understanding. Trial results show that the proposed recieving wire has high increase of 30.0 dBi at 21GHz, gap effectiveness of 40% and 1-dB gain data transmission of 9.6% (20.1GHz-22.2GHz). The proposed twofold layer transmit cluster reception apparatus incredibly disentangles the structure multifaceted nature and lessens the thickness, the mass, and the expense as for existing transmit exhibit radio wires.

Index Terms— Transmit array antenna, two degrees of freedom (TDF), double-layer, wideband.

1.INTRODUCTION

Recently, transmit array antennas get more and more attention. The idea for transmit array antennas originates from the lens and microstrip array, which has the advantages of high efficiency, high gain, low profile and light weight. Transmit arrays are generally composed of four-layer dielectric substrates. The horn antenna is placed as the feed behind the array. When the feed illuminates the array, different elements achieve different phase shifts and uniform transmission magnitude. By arranging

array elements, a desired radiation pattern can be obtained. Compared with reflect array antennas, transmit array antennas eliminate the effects of feed blockage, which can decrease aperture efficiency and gain. Meanwhile, transmit array can be conformable to the equipment. In general, both the 1-dB gain bandwidth and aperture efficiency are adopted for evaluating antenna performance. The 1-dB gain bandwidth means the bandwidth when the gain is greater than the maximum gain minus 1db. The aperture efficiency is defined as the ratio of the measured gain to the maximum directivity. 7.5% 1-dB gain bandwidth has been

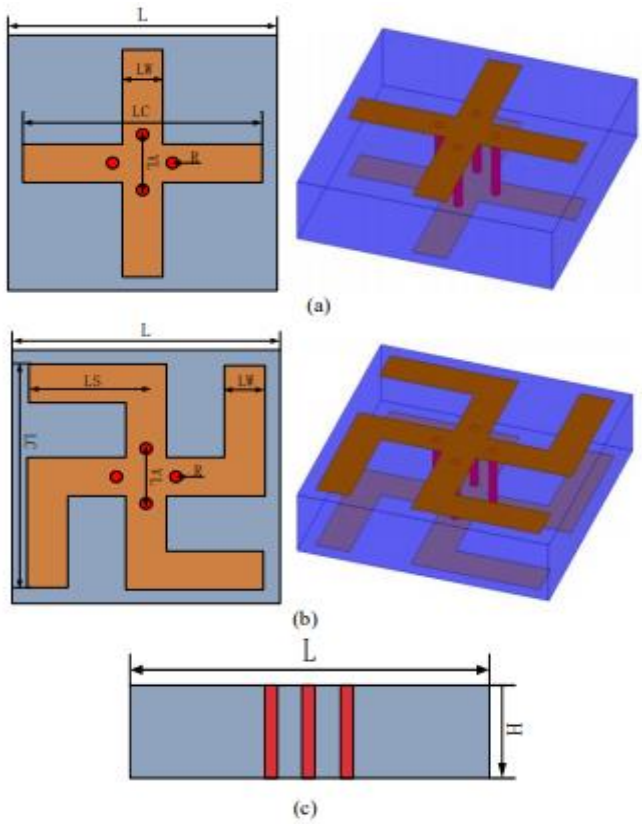

Fig 1.1 Configuration of the proposed transmit array element. (a) design I: cross-dipole element (top view and 3D view) (b)design II: spiral-dipole element (top view and 3D view) (c) side view.

presented. Obviously, the four-layer transmit array antenna using a dual-resonant square element does not realize the wideband performance. In order to improve the 1-dB gain bandwidth, a method of controlling the phase and magnitude on the aperture is proposed. Bandwidth improvement can be achieved by using the proposed techniques in the article and 1-dB gain bandwidth has reached 9.8% and 11.7%, respectively. In, a novel element without any dielectric substrate is proposed. The element comprises three thin metallic layers with air gap. The transmit array has 1-dB

gain bandwidth of 9.6% and peak efficiency of 55%. The peak efficiency is defined as the largest aperture efficiency in 1-dB gain bandwidth. In, a wideband dual linearly polarized transmit array antenna is designed, fabricated and measured. Simulation and measurement results have good agreement. In a recent report, a wideband linearly polarized transmit array is proposed at V-band(57-66GHz). None of the antennas mentioned above gets rid of multi-layer structure, which increases the thickness, the mass and the cost. The design of double-layer wideband transmit array antennas is an important topic of research. In addition to the wideband characteristic, high efficiency is also an attractive feature. A triple-layer transmit array antenna.

2.LITERATURE SURVEY

2.1 J. G. Nicholls, S. V. Hum, "full-space electronic beam-steering transmitarray with integrated leaky-wave feed," IEEE Trans. Antennas Propag.,vol.64,no.4,pp. 1473–1481, 2016.

A new low-profile, full-space, electronic beam-steering antenna architecture which combines the full-space beam-steering properties of reconfigurable transmitarrays with the low-profile feeding characteristics of leaky-wave antennas is proposed. The design uses an integrated leaky-wave feed to spatially distribute power across a reconfigurable transmitarray aperture in a low-profile manner while individual element phase control using varactor diodes enables full-space pencil-beam-steering. A 6×6 element array was fabricated and experimentally verified, and full-space (both azimuth and elevation) beam-steering was demonstrated at angles up to 45° off broadside with a total efficiency for all scan angles on the order of 25%-35%. The design demonstrates a tenfold reduction in the overall thickness over the original transmitarray, improved aperture amplitude distribution control, as well as improved spillover control. The design also acts as a lower cost, scalable alternative to phased arrays as it does not require a complicated beamforming network and the feed and aperture are easily scaled.

2.2 H. Nematollahi, J-J Laurin "design of broadband transmitarray unit cells with comparative study of different numbers of layers," IEEE Trans. Antennas Propag.,vol.63,no.8,pp. 3410–3422, 2015.

A generalized methodology to design low-profile transmitarray (TA) antennas made of several stacked layers with nonresonant printed phasing elements is presented. A

study of the unit cell bandwidth, phase-shift range and tolerances has been conducted considering different numbers of layers. A structure with three metalized layers with capacitive and inductive elements enabling a phase range of nearly 360° and low insertion loss is introduced. A study of the four-layer structure shows improvement in the performance of the unit cells in terms of bandwidth from 2% to more than 20% and a complete phase coverage. Implementations on a flexible substrate of TAs with progressive phase shift operating at 19 GHz are used for validation.

3.PROPOSED SYSTEM

3.1 Element Structure

Three-dimensional structure of the proposed element is depicted in Fig. 4.1(a-c). The proposed element is manufactured on dielectric substrate with relative permittivity εr and loss tangent δ. The overall dimensions of the element are L×L×H. Fig.3.1 shows the design I and Fig. 3.2 shows the design II. We define the length of LC as the first degree of freedom (FDF) and the length of LS as the second degree of freedom (SDF). When LC varies from 4mm to 8mm and LS varies from 0.6mm to 4mm, the FDF and SDF cases can adjust the 300-degree and 130-degree phase shift range, respectively. The FDF achieves the start degree of phase shift range, the SDF completes the last

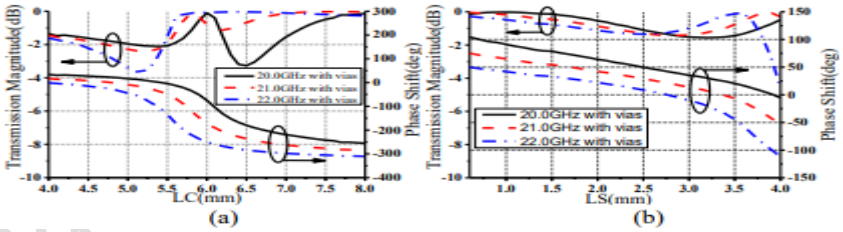

Fig 3.1 Transmission magnitude and phase of the unit cell. (a) transmission magnitude and phase of FDF with vias (b) transmission magnitude and phase of SDF with vias.

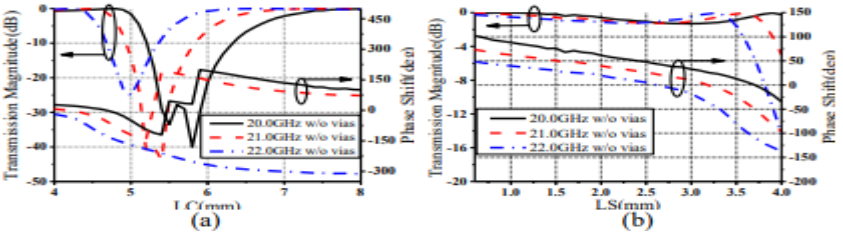

Fig 3.2 Transmission magnitude and phase of the unit cell. (a) transmission magnitude and phase of FDF without vias (b) transmission magnitude and phase of SDF without vias.

degree of phase shift range. If the element needs phase compensation within 300 degrees, cross-dipole is used as the design unit showing in Fig. 4.1(a). If the compensation phase is between 300 degrees and 360 degrees, the spiral-dipole is used as the design element showing in Fig. 4.1(b). By combining these two parameters, we get a 360-degree phase shift range. four metal vias passing through the entire dielectric substrate are used to enhance the coupling strength. Detailed dimensions of the proposed element are given in Table I.

3.2 Two Degrees of Freedom

Model simulation uses master-slave boundary conditions to simulate an infinite number of array elements. When the proposed element operates at 21 GHz, the FDF achieves 300-degree phase shift range, as shown in Fig.2(a), with the parameter LC varying from 4 to 8mm; Fig. 4.2(b) shows the phase shift of the SDF. When parameter LS varies from 0.6mm to 4mm, 130-degree phase shift is achieved, which indicates that the TDF totally achieves 360-degree phase shift range. The reason for employing cross-dipole and spiral-dipole element is that both elements have low space utilization and belong to similar units. The cross-dipole unit can be continuously changed to a spiral-dipole unit, which is a prerequisite for realizing TDF in a limited space. There is a high consistency of phase shift in the band from 20GHz to 22 GHz in Fig. 2. The phase shift curves are basically parallel to each other. We finally get a desired phase shift range with a smooth slope, which is the reason why the element has broadband characteristic. Due to the introduction of TDF, the proposed unit obtains sufficient phase shift range. The compensation phases are implemented by changing the length LC from 4 to 8mm and the length LS from 0.6 to 4mm with a resolution of 0.02mm. The current processing accuracy is generally 0.01mm. TDF will play an important role in designing transmit array antennas. Normally, the proposed element needs to receive incident waves at different incident angles. Therefore, it is significant to

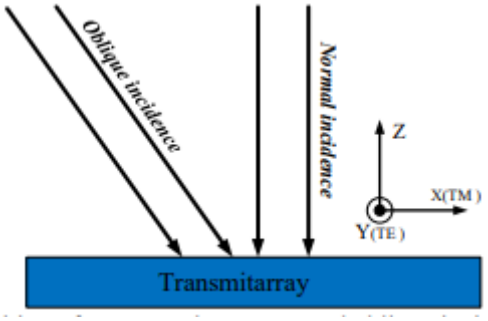

Fig 3.3 The definition of TM, TE plane wave and oblique incident.

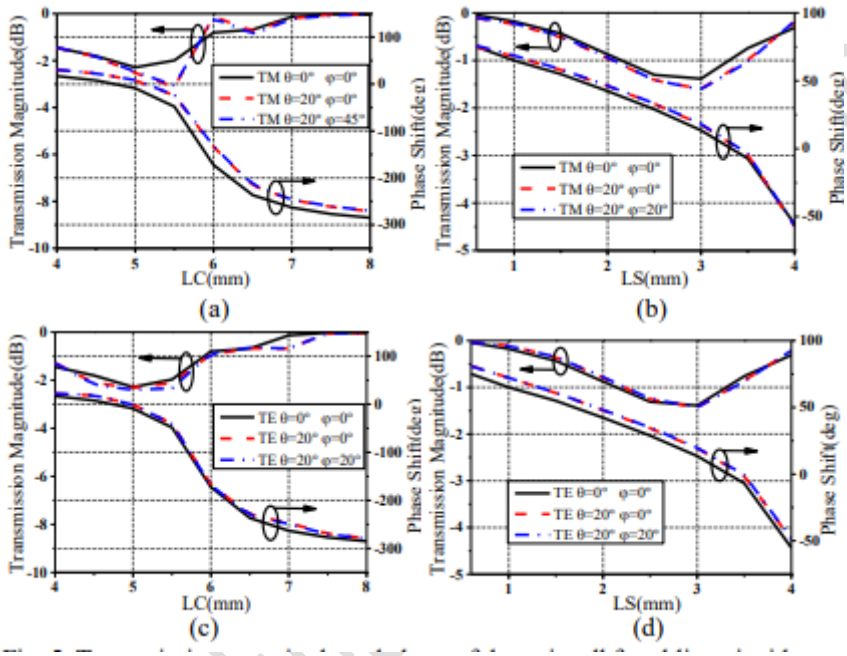

Fig 3.4 Transmission magnitude and phase of the unit cell for oblique incidence. (a) FDF for TM plane wave (b) SDF for TM plane wave (c) FDF for TE plane wave (d) SDF for TE plane wave.

calculate the transmission magnitude and phase at different incident angles. According to the distance between the horn and the transmit array as well as the side length of the transmit array, the maximum incident angle is 18.5 degrees and the elevation angle of 0° and 20°is simulated to verify the transmission magnitude and phase with TE and TM plane waves. The definition of TM and TE plane waves is given in Fig.4. The simulation results are shown in Fig.5(a-b) and Fig.5(c-d), respectively. Transmission magnitude and phase are almost the same when the oblique angle is less than 20°. However, the phase deviation becomes apparent when the incident angle increases. The reason is as follows: when the incident angle is more than 0°, the upper metal patch covers the lower patch, which leads to the inconsistency. The phase deviation is bad for transmit array antenna. In fact, the

maximum phase difference is less than 18°, which does not affect the transmit array design.

3.3 Analysis of working principle

Fig.3(a) shows the variation of transmission magnitude and phase without metal vias. The transmission magnitude fault occurs when the length LC varies from 5mm to 7mm. The proposed element reflects most of the energy from the horn antenna, which directly leads to the phase jump. Compared with Fig. 2(b), the transmission magnitude and phase is basically the same in Fig. 3(b). Therefore, it must be pointed out that metal vias are necessary for the first degree of freedom. The current distribution of the element is presented in Fig.6. Due to the symmetry of the element structure, only the current distributions under TM plane wave are analysed. Fig.6(a) shows the current distribution of the cross-dipole element. The

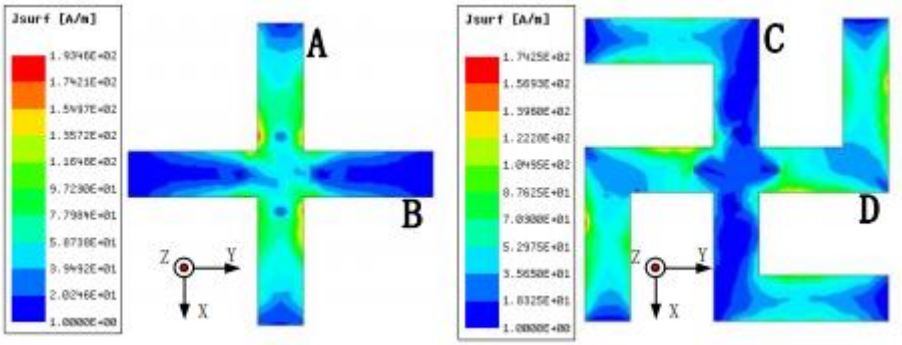

Fig 3.5 Current distribution of the proposed element at 21GHz. (a) top view of FDF (b)top view of SDF.

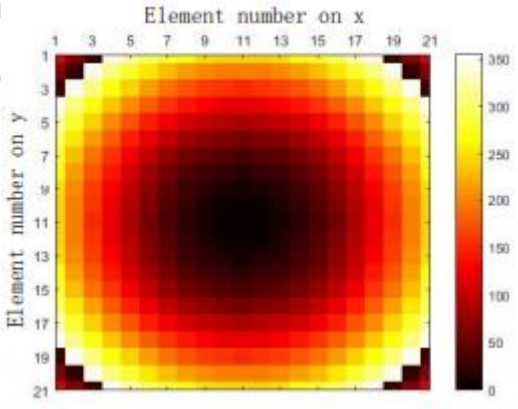

Fig 3.6 The phase shift distribution of all elements.

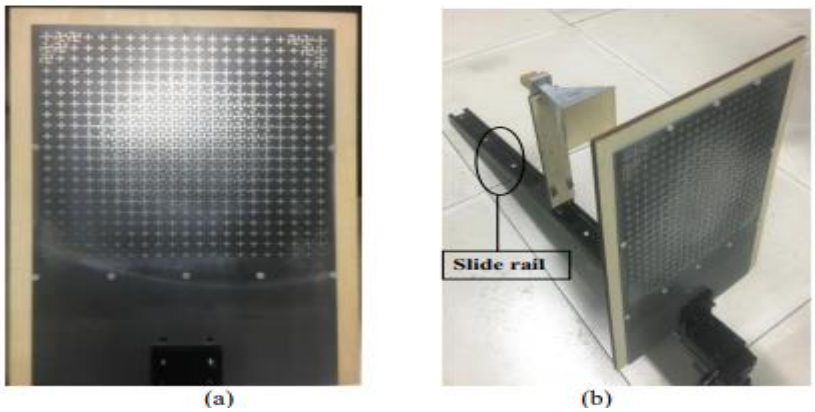

Fig 3.7 Fabricated transmit array. (a) Top layer. (b) overall structure.

current appears in the vertical direction only. Therefore, the length of the patch A affects the phase shift. FDF works here and it completes the start degree of phase shift range. The current distribution of the spiral-dipole element is presented in Fig.6(b). Almost all current is transferred to patch D. SDF increases the current path length of patch D and affects the phase shift. The last degree of phase shift range is achieved by SDF.

3.4 Configuration and Optimization of the Transmit array

The antenna prototype is shown in Fig. 8. The diameter of the circular aperture is 338 mm. Since the feed blockage effect does not exist in the transmission mode, the prime feeding configuration is utilized. A vertically polarized corrugated horn located 420 mm above the transmit array aperture is employed as the primary feed. Its simulated gain is 18.1 dBi and a simple cosq (θ) model with a matching q factor of 15.5 is used to facilitate the computation. With the chosen element spacing of 6.5 mm, the total number of elements is 2032. The phase shift of each element is then calculated using the ray tracing method [18] to compensate for the spatial path delay associated with the feed and collimate the beam in the boresight direction.

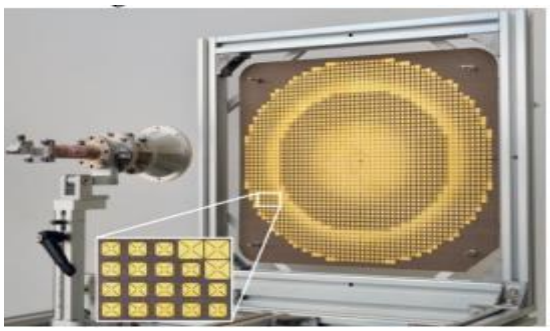

Fig 3.8 Prototype of the Ka-band transmit array using the proposed elements.

The transmit array is calculated using the array theory method [19]. The calculated radiation pattern is shown in Fig. 9, where the gain at 20 GHz is 34.0 dBi, with aperture efficiency of 50%, illumination efficiency of 79%, spill over efficiency of 87%, and loss efficiency of 73%.

The prototype is tested in a compact-range anechoic chamber, and the measured pattern is also plotted in Fig. 9. The measured main beam and first side lobe are in good agreement with the simulation. The measured first sidelobe and cross-polarization levels are 22.5 dB and 28.0 dB lower than the main beam, respectively. The measured gains within the frequency band of interest are shown in Fig. 10, which is 33.0 dBi at 20 GHz with aperture efficiency of 40%. The measured 1-dB gain bandwidth is 5.9%. The calculation and experimental results of the prototype transmit array successfully validate the radiation performance of the proposed double-layer transmit array element.

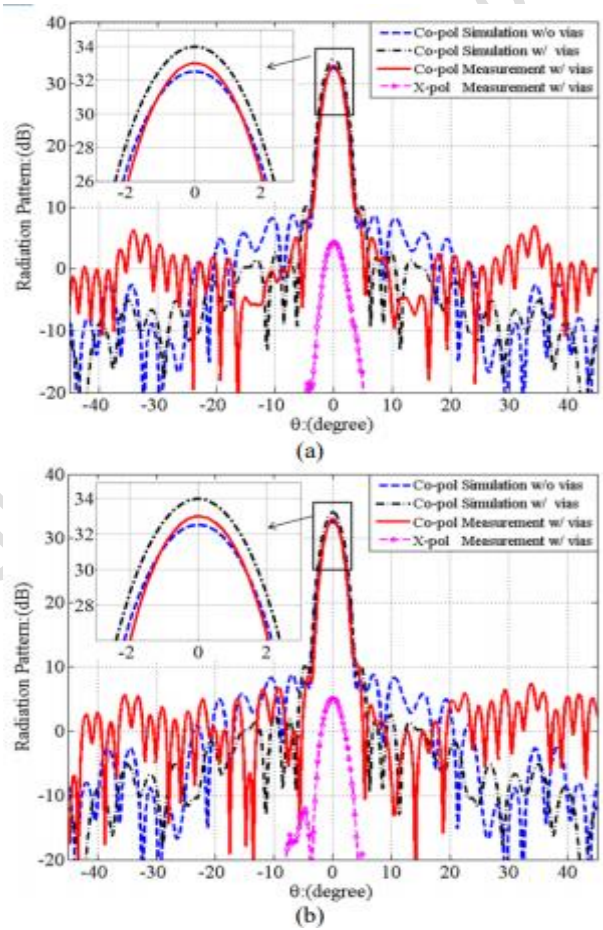

Fig 3.9 Calculated and measured radiation patterns: (a) E-plane; (b) H-plane.

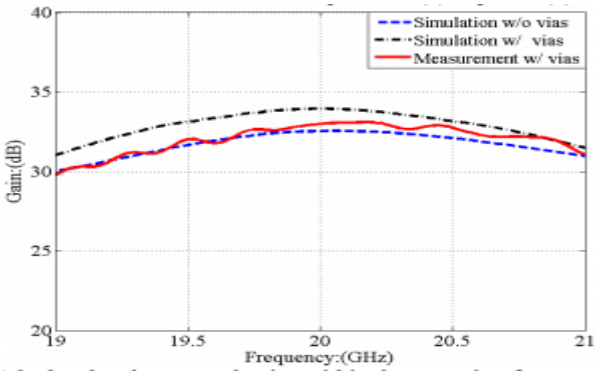

Fig 3.10 Calculated and measured gains within the operating frequency band.

Certain discrepancy exists between calculated and measured results in terms of gain and sidelobe level. The difference between calculated and measured gains is 1.0 dB, and the sidelobe levels beyond ±20° angular range are higher than calculation. The primary reasons for the discrepancy are as follows. Firstly, the predicted radiation pattern is calculated using the array theory method, so no back radiation is taken into account in the calculation, leading to artificially higher calculated gain.

The sidelobes in the far angular region are also lower than the actual values. Secondly, due to the limitation on fabrication technique, the right angles of the slots are rounded in the fabricated prototype, which effectively reduces the slot length, resulting in certain phase errors. Lastly, the frame to support the transmit array aperture is made of aluminium. Its size and thickness are relatively large, the diffraction from which could cause higher sidelobes and gain loss. To clarify the impact of vias, the calculated pattern and gain of the same reflect array configuration using elements without vias are also plotted in Figs. 9 and 10. Compared with that using the proposed elements with vias, a noticeable gain loss of about 1.5 dB is resulted due to the limited phase range.

To demonstrate the effectiveness of the proposed design, this work is compared with some of the latest publications on transmit arrays and the performances are summarized in Table I. The 4-layer M-FSS type design achieves good gain and aperture efficiency performances at the price of complex structure and high cost. This work achieves better phase range and aperture efficiency compared with the 2- or 3-layer M-FSS type designs. Hence, the proposed element design is able to maintain good phase and magnitude characteristics to produce comparable, even better radiation performances as conventional transmit arrays. This novel design significantly simplifies the structure of transmit array elements. The two-layer patches can be etched on a single layer of laminate using PCB technology, which remarkably

reduces the thickness, mass, and cost of a transmit array. The complexity of fabricating transmit arrays may become comparable to reflect arrays, which hopefully can stimulate the transmit array applications.

Table 4.1 Comparison of The Proposed Transmit Array with Referenced Designs

Ref.	Freq. (GHz)	Number of Layers	Phase Range	Gain (dB)	Aperture Efficiency
This work	20	2	305 °	33.0	40%
7	6	2	170 °	16.7	23.4%
5	11.3	3	270 °	28.9	30%
6	13.5	4	360 °	30.22	50%

4.RESULTS AND DISCUSSIONS

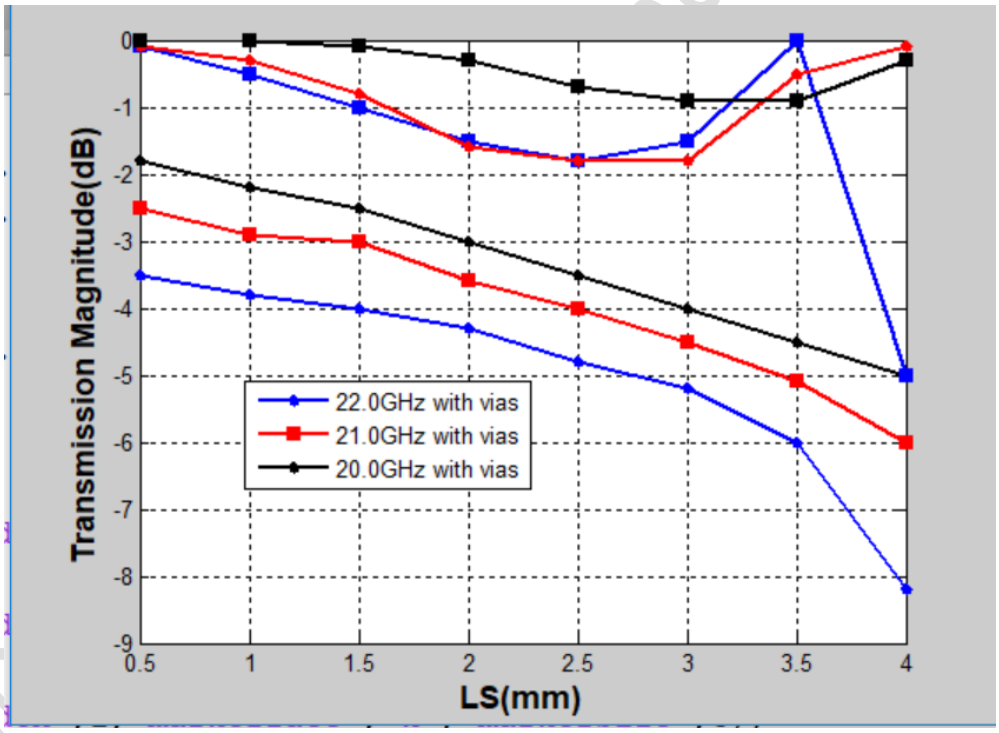

Fig 4.1: transmission magnitude and phase of SDF with vias.

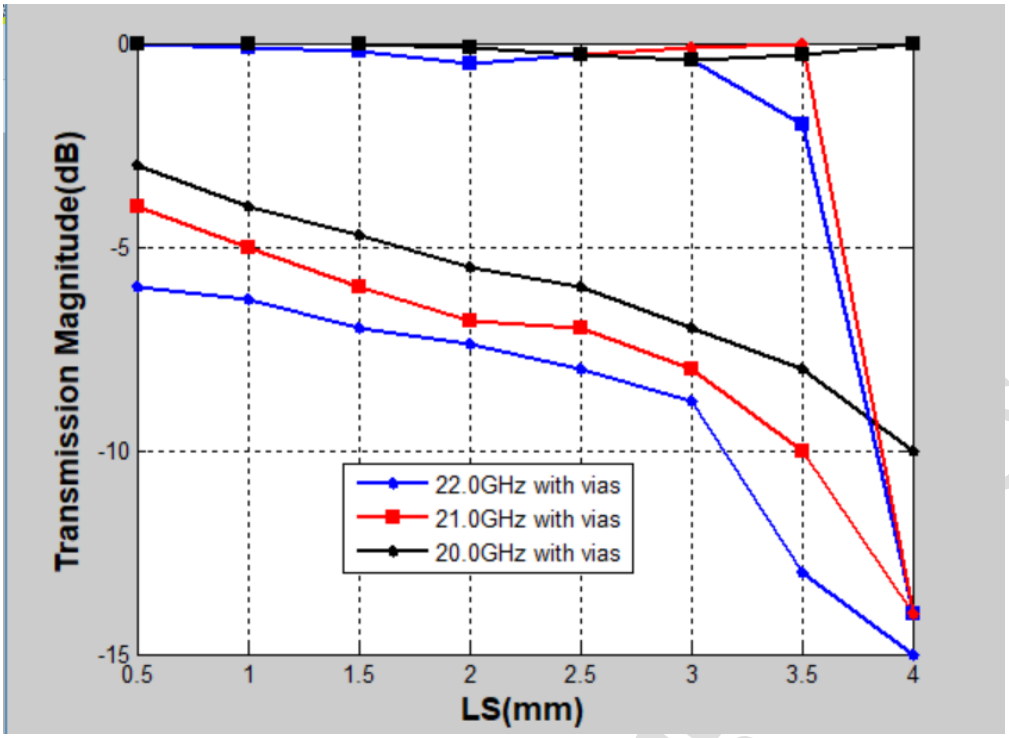

Fig 4.2: transmission magnitude and phase of SDF without vias.

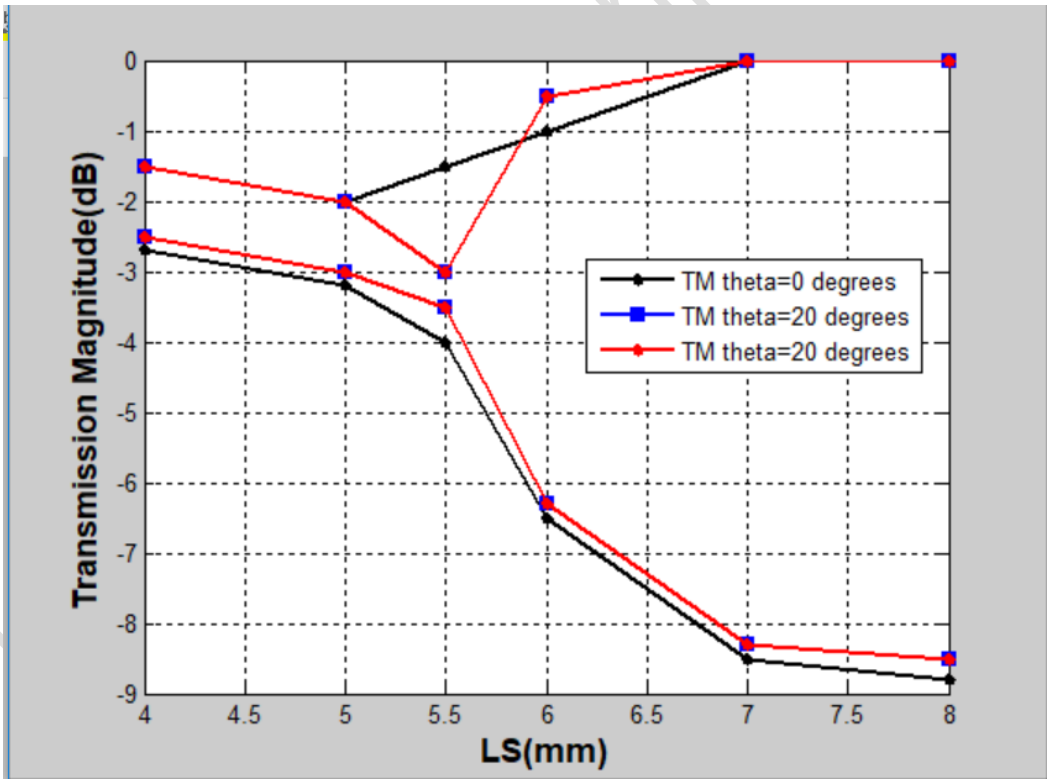

Fig 4.3: SDF for TM plane wave.

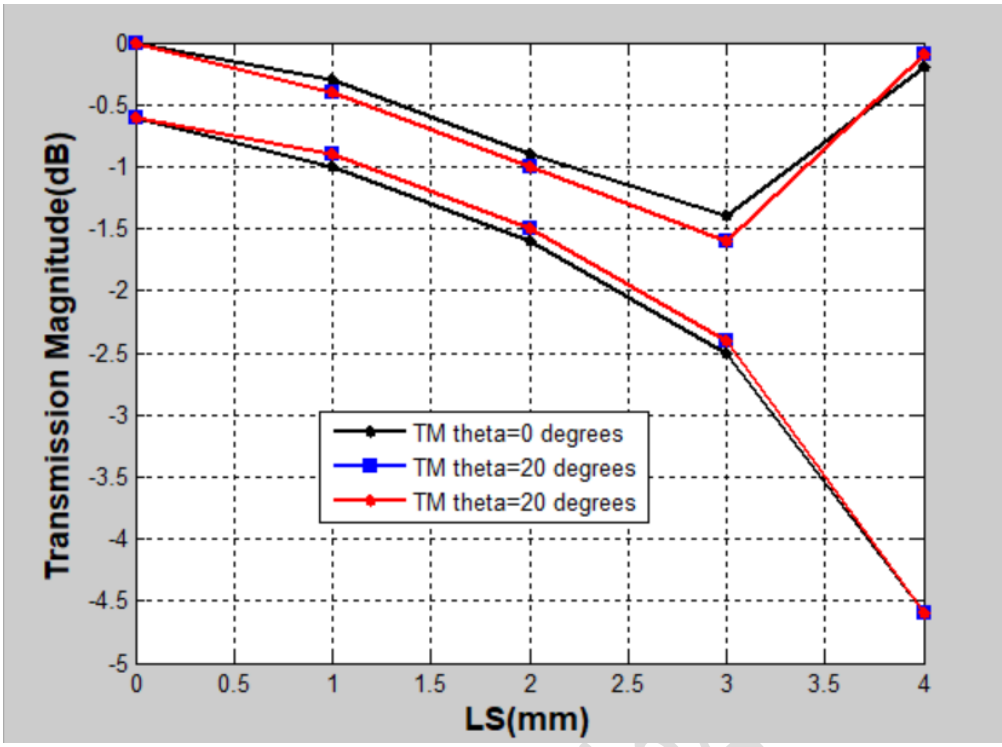

Fig 4.4: SDF for TE plane wave.

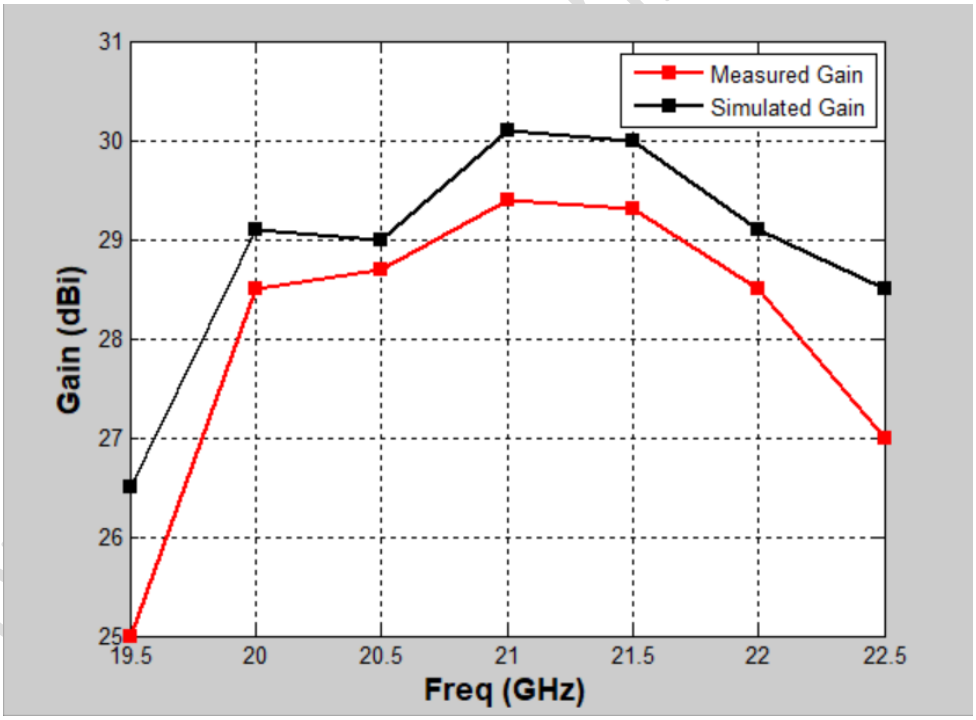

Fig. 4.5. The comparison between simulated and measured gain versus frequency.

4.1 Simulation and Experimental Results

A soft HFSS V15 software is adopted to simulate the transmit array antenna. The simulated gain and radiation efficiency are 30.5dBi and 50%, respectively. Fig. 8 shows the fabricated transmit array antenna. The prototype was measured in a microwave anechoic chamber, and the measurement results are shown in Fig.9(a-c). The main lobe and the first sidelobe regions of the measurement patterns substantially coincide with the simulated patterns. However, it is obvious that the other sidelobes are lower than the simulation results, which is caused by the feed alignments error, the permittivity deviation and intrinsic noises in the anechoic chamber. The antenna has sidelobe level of 14dB and cross-polarization level of 26dB within the 1-dB gain bandwidth. The comparison between simulated and measured gain versus frequency is presented in Fig. 10. The measured gain is approximately 0.6 dBi smaller than the simulated gain.

The discrepancy is mainly caused by the PCB fabrication error, phase centre misalignment and scattering of metal rails. The measured 1-dB and 3-dB gain bandwidths are 9.6% and 16.7%, respectively. The measured aperture efficiency at the centre frequency is 40%. The simulation and measurement results demonstrate the excellent radiation characteristics of the proposed element. Table 5.1 lists the characteristics of the proposed antenna and the recent published antennas. It can be concluded that the proposed element possesses better performances than all existing unit in the table. The most fundamental reason is that TDF provides sufficient phase shift range in the case of double-layer structure. The article only explores the case of TDF, and the study of multiple degrees of freedom has not been implemented yet. It is obvious that multiple degrees of freedom make the element obtain better performance.

5.CONCLUSION

A novel double-layer wideband transmit array element using two degrees of freedom is proposed in this communication. The two degrees of freedom realize 360-degree phase shift range. The superior performance of the proposed element is presented, and a transmit array is designed, fabricated, and measured to validate the element characteristics. Simulation and measurement results are in good agreement, and the measured gain of 29.4 dBi with aperture efficiency of 40% is obtained at 21GHz. Experimental results show that the proposed antenna has a 1-dB gain bandwidth of 9.6% (20.1GHz-22.2GHz). With the double-layer structure, the

proposed transmit array antenna greatly simplifies the design complexity and fundamentally solves the problems of thickness, mass, and cost.

REFERENCE

[1] S. Datthanasombat, L. R. Amaro, J. A. Harrell, S. Spitz and J. Perret, Layered lens antenna, IEEE Antennas and Propagation Society International Symposium, pp. 777–780, Boston, 2001. DOI: 10.1109/aps.2001.959839. 3, 25, 33, 34, 57, 62, 69, 139

[2] A. H. Abdelrahman, F. Yang, and A. Z. Elsherbeni, Transmission phase limit of multilayer frequency selective surfaces for transmitarray designs, IEEE Transactions on Antennas and Propagation, vol. 62, no. 2, pp. 690–697, 2014. DOI: 10.1109/tap.2013.2289313. 3, 25, 33, 34, 36, 70, 96, 139

[3] R. Milne, Dipole array lens antenna, IEEE Transactions on Antennas and Propagation, vol. AP-30, no. 4, pp. 704–712, 1982. DOI: 10.1109/tap.1982.1142835. 33, 57, 69

[4] C. G. M. Ryan, M. Reza, J. Shaker, J. R. Bray, Y. M. M. Antar, and A. Ittipiboon, A wideband transmitarray using dual-resonant double square rings, IEEE Transactions on Antennas and Propagation, vol. 58, no. 5, pp. 1486–1493, 2010. DOI: 10.1109/tap.2010.2044356. 33, 39, 62, 69, 70, 95

[5] M. A. Al-Joumayly and N. Behdad, Wideband planar microwave lenses using subwavelength spatial phase shifters, IEEE Transactions on Antennas and Propagation, vol. 59, no. 12, pp. 4542–4552, 2011. DOI: 10.1109/tap.2011.2165515. 33

[6] M. Li, M. A. Al-Joumayly, and N. Behdad, Broadband true-time-delay microwave lenses based on miniaturized element frequency selective surfaces,IEEE Transactions on Antennas and Propagation, vol. 61, no. 3, pp. 1166–1179, 2013. DOI: 10.1109/tap.2012.2227444. 3, 33, 95

[7] D. M. Pozar, Flat lens antenna concept using aperture coupled microstrip patches, Electronic Letters, vol. 32, no. 23, pp. 2109–2111, 1996. DOI: 10.1049/el:19961451. 4, 95

[8] H. J. Song and M. E. Bialkowski, transmit array of transistor amplifiers illuminated by a patch array in the reactive near-field region, IEEE Transactions on Microwave Theory and Techniques, vol. 49, no. 3, pp. 470–475, 2001. DOI: 10.1109/22.910550.

[9] P. Padilla de la Torre and M. Sierra-Castaner, Design and prototype of a 12-GHz transmitarray, Microwave and Optical Technology Letters, vol. 49, no. 12, pp. 3020–3026, 2007. DOI: 10.1002/mop.22950. 24

[10] H. Kaouach, L. Dussopt, R. Sauleau, and T. Koleck, X-band transmit-arrays with linear and circular polarization, 3rd European Conference on Antennas and Propagation, EuCAP, pp. 1191–1195, Berlin, Germany, 2009. 69

AUTHOR'S PROFILES

T.Prasanna received her B.Tech Degree in Electronics and Communication Engineering at Gokula Krishna College of Engineering, Sullurpet, affliated to JNTUA, Ananthapuramu. And Persuing M.Tech Degree in Digital Electronics and Communication Systems at Gokula Krishna College of Engineering, Sullurpet. Her areas of interest are communication systems and digital signal processing.

M. Gnanapriya received her B.E degree in the field of Electronics and Communication Engineering from Madurai Kamaraj University and completed her M.E in the field of Computer science from AnnaUniversity, Tamilnadu. She is currently working as Associate professor & Head of ECE Dept, Gokula Krishna College of Engineering. Her areas of interest are Digital Signal Processing, Digital Image processing and Embedded Systems.